Electronic Supplementary Information (ESI)

Influence of Polycation Modification on Droplet Size and Internal Structure in RNA/ Poly-L-Lysine Coacervates

Alba Ledesma-Fernandez [a], Victor Krivenkov [a,b], Yury Rakovich [a,b,c,d] and Paula Malo de Molina* [a]

a. Centro de Física de Materiales (CFM-MPC), CSIC-EHU, 20018 Donostia-San

b. Polymers and Materials: Physics, Chemistry and Technology, Chemistry Faculty, University of the Basque Country (UPV/EHU), 2018 Donostia-San Sebastián, Spain

c. Donostia International Physics Center(DIPC), 2018 Donostia-San Sebastián

d. IKERBASQUE – Basque Foundation for Science, 48009 Bilbao, Spain.

*p.malodemolina@ehu.eus

Table S1. The main molecular components used in this study — Poly-L-lysine (PLL), RNA, Bis(sulfosuccinimidyl) suberate (BS³), 2 5-dioxopyrrolidin-1-yl acetate (DPA), NHS-Fluorescein, and NHS-Rhodamine.

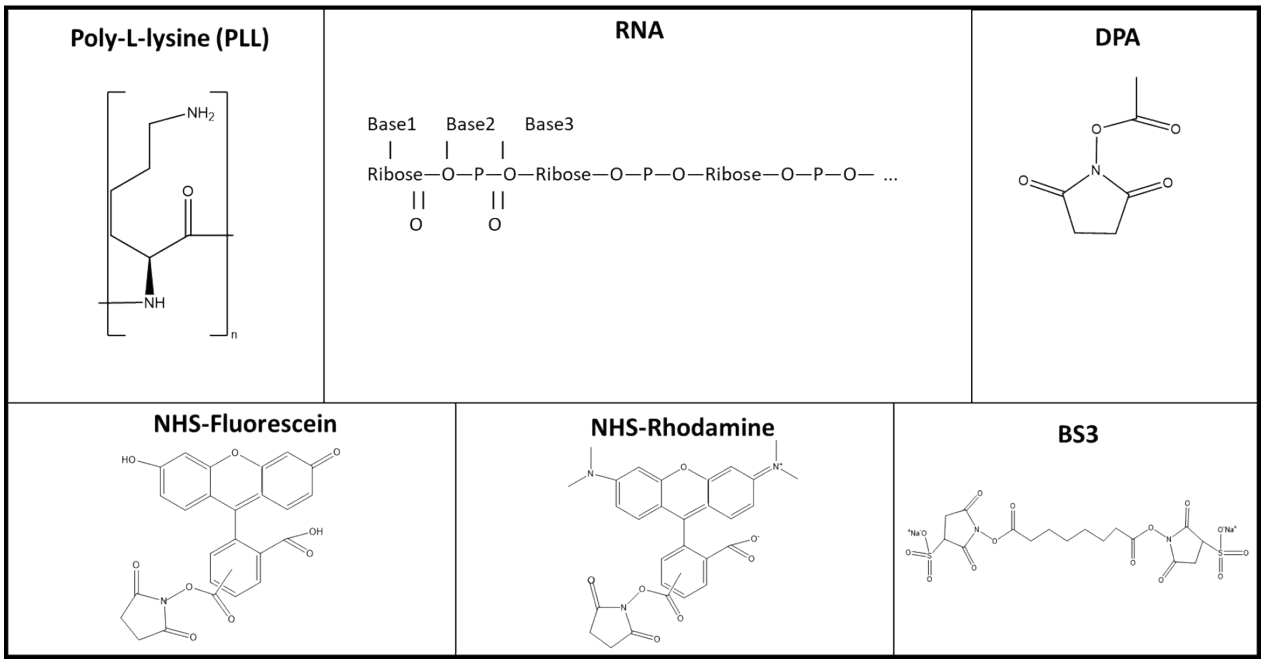

[1]H-NMR spectroscopy of acetylated poly-L-lysine

The characteristic signals of the lysine side-chain methylene groups (δ ≈ 2.85 ppm) and the acetate methyl protons (δ ≈ 3.0 ppm) were integrated to quantify the degree of modification. The appearance of the acetate resonance confirms the covalent attachment of acetyl groups to the poly-L-lysine ε-amines.

The degree of amine modification was calculated from the relative integrals of these peaks according to:

$$\%\, modification\ of\ PLL = \frac{I_{2.85}}{I_{2.85} + I_3} * 100$$

Based on these integrations, the calculated degree of amine modification was 31 % for acetylated PLL and 39% for PLL-NPs.

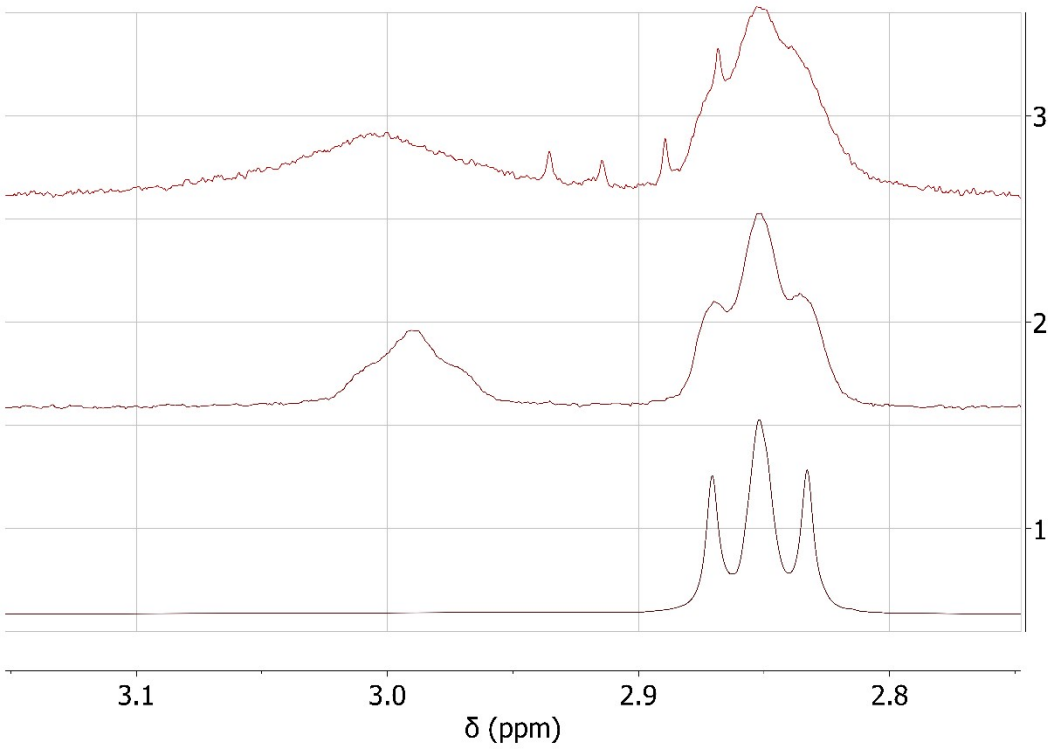

Figure S1. ^{1}H NMR spectrum of poly-L-lysine (PLL) bare (**1**) reacted with 2,5-dioxopyrrolidin-1-yl acetate (NHS-acetate) (**2**) and reacted with BS3 (bis(sulfosuccinimidyl)suberate) (**3**) in D_2O.

Fluorescent labelling of RNA and PLL

The systems studied linear PLL/RNA complexes, PLL-NPs/RNA, and modified PLL/RNA. Fluorescent labelling of the PLL and RNA was performed by mixing the biopolymer solutions in TRIS buffer (10 mM Tris, 0.5 M NaCl, 0.1 mM EDTA, pH 7.6) with NHS-Rhodamine (5/6-carboxytetramethylrhodamine succinimidyl ester, mixed isomers) or NHS-Fluorescein (5/6-carboxyfluorescein succinimidyl ester, mixed isomers) respectively in DMSO at a 1:1 molar ratio (dye:biopolymer). Labelling reactions were carried out for 1 hour at room temperature in the dark under gentle agitation. Unreacted dye was removed using Amicon Ultra centrifugal filters with a 30 kDa molecular weight cutoff. Prior to confocal imaging, fluorescence emission of the labelled samples was measured using a fluorimeter (Cary Eclipse Fluorescence Spectrometer) in order to determine optimal excitation and emission parameters for microscopy. The emission maxima used for imaging were ~ 520 nm for NHS-Fluorescein (excitation at 495 nm) and ~ 580–590 nm for NHS-Rhodamine (excitation at 552 nm), and were adjusted accordingly on the microscope settings (Figure S4).

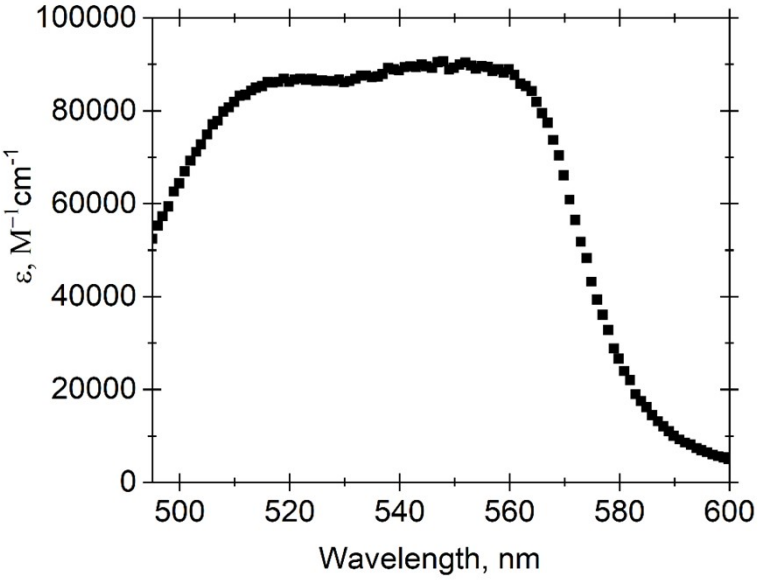

Figure S2. UV–vis absorption (extinction) spectrum of Rhodamine. This spectrum was used as the acceptor absorption spectrum ε_A(λ) for calculation of the spectral overlap integral in the Förster resonance energy transfer (FRET) analysis.

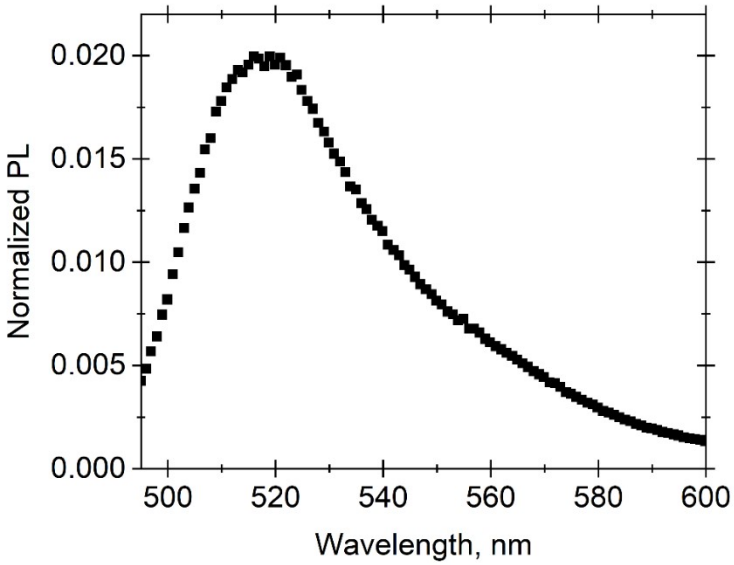

Figure S3. Fluorescence emission spectrum of Fluorescein upon excitation at 495 nm. This spectrum was used as the donor emission spectrum for calculation of the spectral overlap integral in the Förster resonance energy transfer (FRET) analysis.

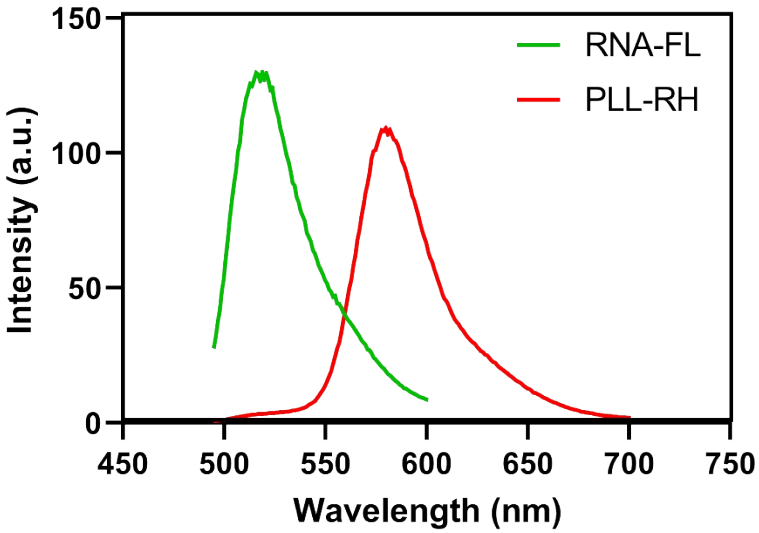

Figure S4. Fluorescent labelling of RNA and PLL was carried out in TRIS buffer using NHS-Fluorescein (green) and NHS-Rhodamine (red), 1:1 molar ratio, dye:biopolymer for 1 h at room temperature in the dark. Unreacted dye was removed by centrifugal filtration (30 kDa MWCO).

Instrument Response Function

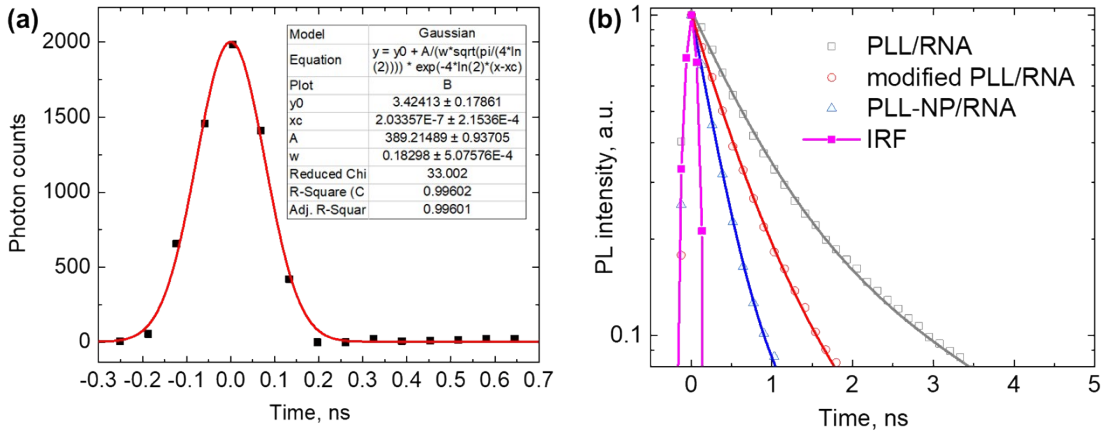

Figure S5. Contribution of the instrument response function (IRF) to the PL decay measurements. (a) IRF; (b) Shortest PL decay kinetics together with IRF.

Homo-FRET control

To evaluate whether the fluorescence lifetime reduction observed in the coacervates could arise from RNA–RNA interactions, self-quenching, or homo-FRET between fluorescein molecules at high local RNA concentration, control experiments were performed using fluorescein-labelled RNA mixed with unlabeled PLL under identical coacervate preparation

conditions (50:50 mass ratio). Confocal microscopy confirmed the formation of coacervate droplets comparable to those observed in the dual-labelled systems. Representative fluorescence lifetime decay curves measured within the droplet regions are shown in Figure S5. The measured fluorescein lifetime in these donor-only coacervates remained approximately 3.3 ns, comparable to the lifetime measured for fluorescein-labelled RNA in the absence of PLL. This indicates that phase separation and high local RNA concentration alone do not produce significant fluorescence lifetime shortening under the conditions studied.
These control experiments therefore suggest that the pronounced lifetime reductions observed in the dual-labelled coacervates primarily arise from interactions between fluorescein-labelled RNA and rhodamine-labelled PLL, consistent with efficient donor–acceptor quenching/FRET associated with closer RNA–PLL proximity.

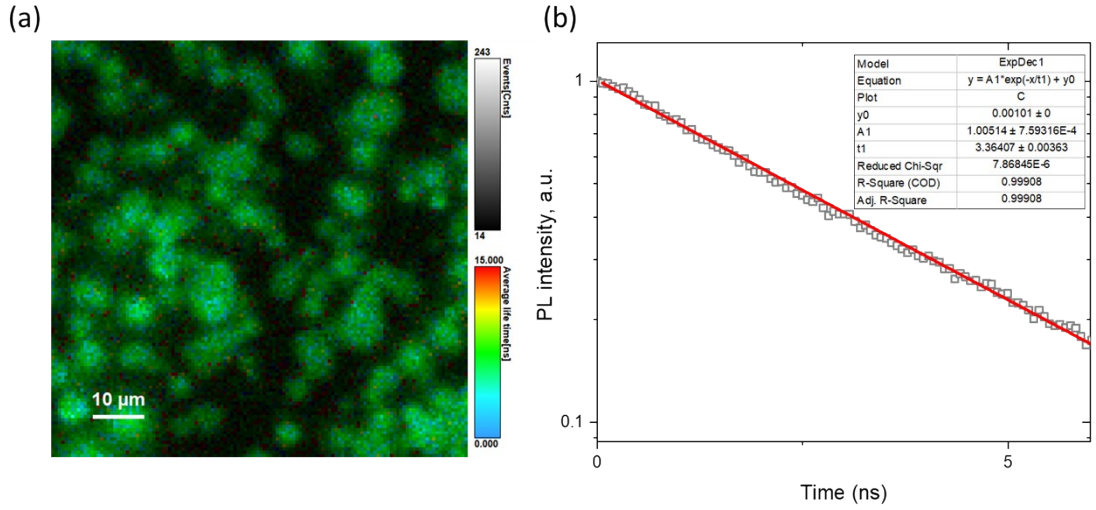

Figure S6. Control fluorescence lifetime measurements of donor-only coacervates formed by mixing fluorescein-labelled RNA and unlabeled PLL·HBr using a 1:1 volume ratio of stock solutions (both at 3 mg mL^{-1}). (a) Confocal fluorescence lifetime image of the coacervate droplets recorded in the fluorescein channel. The color scale corresponds to the average fluorescence lifetime and the intensity scale indicates detected photon counts. (b) Representative fluorescence lifetime decay curve measured within the droplet regions together with the corresponding fit. The extracted fluorescein lifetime (~3.36 ns) remains comparable to that of fluorescein-labelled RNA in the absence of rhodamine-labelled PLL, indicating that coacervation and high local RNA concentration alone do not produce significant fluorescence lifetime shortening under the experimental conditions.

Fluorescence resonance energy transfer distance analysis

To calculate the Forster distance we used the following equations from the ref.[1]. The main parameter characterizing the fluorescence energy transfer (FRET) is its efficiency (*E*). Physically, FRET efficiency is a ratio of rate of relaxation of donor excited state attributed to

FRET (k_{FRET}) to the sum of k_{FRET}, radiative relaxation rate (k_r) and all nonraditive relaxation rates (k_{irr}) except FRET:

$$E = \frac{k_{FRET}}{k_{FRET} + k_r + k_{nr}} \quad \text{(S1)}$$

The FRET efficiency was theoretically estimated using the following equation:

$$E = \frac{n_A R_0^6}{n_A R_0^6 + r^6} \quad \text{(S2)}$$

where r is the distance between the donor and acceptor, n_A is the number of bR molecules which can accept energy via FRET from one QD, and R_0 is the Förster distance (in [nm]) defined as the distance at which the FRET efficiency is 50% ; it can be calculated from the following equation:

$$R_0^6 = 8.79 \times 10^{-11}(\kappa^2 n^{-4} \Phi \times J) \quad \text{(S3)}$$

where Φ is the donor QY, κ^2 is the transition dipole orientation factor (we assumed random orientation, and the averaged value of 2/3), N_A is Avogadro's number, n is the refractive index of the medium, and J is the overlapping integral (in [$M^{-1}cm^{-1}nm^4$]) between the QY PL spectrum $F_D(\lambda)$ and bR absorption spectrum $\varepsilon_A(\lambda)$:

$$J = \int_0^\infty F_D(\lambda)\varepsilon_A(\lambda)\lambda^4 d\lambda \quad \text{(S4)}$$

Using the extinction spectrum of rhodamine (Figure S2) and emission spectrum of fluorescein (Figure S3) we estimated J as $6.27 \times 10^{15} M^{-1} cm^{-1} nm^4$ and the FRET distance as $R_0 \sim 6.7\ nm$.

SAXS Fit Residuals for Coacervate Samples

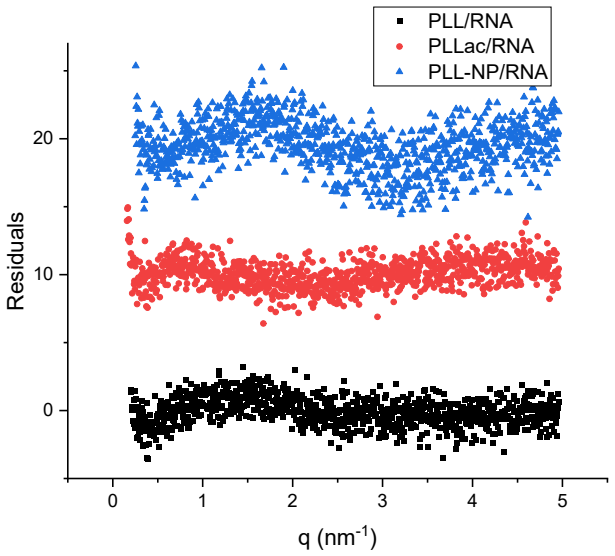

Figure S7. Residuals corresponding to the Ornstein–Zernike fits of the SAXS profiles shown in Figure 4 for the coacervate systems linear PLL/RNA, modified PLL/RNA (PLLac/RNA), and PLL-NPs/RNA. The data were fitted using the OZ expression (eq. 3) to describe concentration

fluctuations and internal chain correlations within the dense coacervate phase, from which the correlation length, ξ, was extracted.

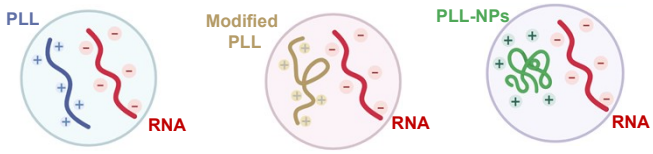

Figure S8. Coacervate systems formed by linear PLL (blue), modified PLL (brown), and PLL-NPs (green) complexed with RNA (red). Well-defined PLL, modified PLL, and PLL-NPs solutions were prepared and subsequently mixed with RNA to form the corresponding coacervates.

References

1 J. R. Lakowicz, in *Principles of Fluorescence Spectroscopy*, Springer US, Boston, MA, 2006, pp. 443–475.